Center for Astrophysics
Preprint Series No. 3198

PERFORMANCE OF SOVIET AND U.S. HYDROGEN MASERS

Adolf A. Uljanov and Nikolai A. Demidov
"Quartz" Research and Production Association, Gorkii, USSR

Edward M. Mattison and Robert F.C. Vessot
Smithsonian Astrophysical Observatory, Cambridge, Massachusetts

David W. Allan
National Institute of Standards and Technology, Boulder, Colorado

and

Gernot M.R. Winkler
United States Naval Observatory, Washington, DC

To be published in *Proc. 22nd Annual Precise Time and Time Interval (PTTI) Applications and Planning Meeting*, 1990

PERFORMANCE OF SOVIET AND U.S. HYDROGEN MASERS

Adolf A. Uljanov and Nikolai A. Demidov
"Quartz" Research and Production Association, Gorkii, USSR

Edward M. Mattison and Robert F. C. Vessot
Smithsonian Astrophysical Observatory, Cambridge, Massachusetts, USA

David W. Allan
National Institute of Standards and Technology, Boulder, Colorado, USA

Gernot M. R. Winkler
United States Naval Observatory, Washington, D.C., USA

ABSTRACT

The frequencies of Soviet- and U.S.-built hydrogen masers located at the Smithsonian Astrophysical Observatory and at the United States Naval Observatory (USNO) were compared with each other and, via GPS common-view measurements, with three primary frequency-reference scales. The best masers were found to have fractional frequency stabilities as low as 6×10^{-16} for averaging times of approximately 10^4 s. Members of the USNO maser ensemble provided frequency prediction better than 1×10^{-14} for periods up to a few weeks. The frequency residuals of these masers, after removal of frequency drift and rate of change of drift, had stabilities of a few parts in 10^{-15}, with several masers achieving residual stabilities well below 1×10^{-15} for intervals from 10^5 s to 2×10^6 s. The fractional frequency drifts of the 13 masers studied, relative to the primary reference standards, ranged from -0.2×10^{-15}/day to $+9.6\times10^{-15}$/day.

INTRODUCTION

A welcome consequence of *glasnost*, the Soviet movement to openness, has been the recent availability of Soviet-built hydrogen masers for testing in the United States. In September 1990, two atomic hydrogen masers built by the Gorkii Instrument-Making Research and Development Institute were shipped to the Smithsonian Astrophysical Observatory (SAO) for comparison with U.S.-built masers and with time scales throughout the world. This unprecedented event was a result of discussions among officials of the U.S. National Institute of Standards and Technology (NIST), the Soviet "Quartz" Research and Production Association, and SAO.

Because of the previous scarcity of information on Soviet masers, the initial and primary interest of the comparisons was on the performance of the Soviet masers; however, for two reasons the scope of the work expanded to include other frequency standards. First, the frequency of a clock cannot be evaluated in isolation, but must be measured relative to accepted primary references; thus it was important to compare the masers at SAO with international time scales. Second, the use of common-view Global Positioning System (GPS) comparisons made it possible to include in the study an ensemble of nine hydrogen masers located at the United States Naval Observatory (USNO). In addi-

tion to being used to extend the TAI time scale over the period of observation, these masers represent a cohort of state-of-the art frequency standards whose performance has not previously been reported on. Thus we have evaluated a substantial number of hydrogen masers produced by manufacturers worldwide.

MASERS STUDIED

Four of the masers under study were located at the SAO Maser Laboratory. Two of these, serial numbers P13 and P26, are model VLG-11 masers built by the SAO Maser Group. The Soviet masers[1,2] at SAO were a model Ch1-75 active maser and a model Ch1-76 passive maser[3]. All masers other than Ch1-76 were active oscillators. Maser Ch1-75 is equipped with an autotuning system designed to stabilize the resonance frequency of the maser's microwave cavity, and thus reduce frequency variations due to cavity pulling. The autotuner, which was operated during part of this study, employs linewidth modulation by means of alternation of the internal magnetic field gradient at intervals of 100 s; a high-stability signal from another maser is used as a reference for the system. Masers P13 and P26 do not use cavity autotuners.

Nine masers at the USNO were studied. Three were SAO VLG-11 masers, serial numbers P18, P19, and P22; two were SAO VLG-12 masers[4], numbers P24 and P25; and four were commercial masers[5], serial numbers N2, N3, N4, and N5.

The masers were compared with each other and with three primary time scales, TAI, NIST(AT1), and UTC(PTB). TAI (International Atomic Time) is maintained by the Bureau International des Poids et Mesures (BIPM) in Sevres, France; it incorporates time and frequency data from about 180 clocks located in more than 50 standards laboratories throughout the world. NIST(AT1) is an unsteered, unsyntonized cesium-generated time scale maintained by the NIST Time and Frequency Division, Boulder, Colorado. Its generating algorithm, AT1, is optimized for frequency stability and minimum time prediction error. UTC(PTB), generated at the Physikalische-Technische Bundesanstalt in Braunschweig, Germany, is controlled by PTB primary cesium standard Cs-1.

TIME AND FREQUENCY COMPARISON SYSTEMS

Several time and frequency comparison systems were employed to link the masers and the time scales, and to provide measurements of frequency stability over both short and long time spans.

Three systems were used at SAO to compare the masers located there (Fig. 1). Frequency difference measurements for intervals of 0.8 s and longer were made with SAO's beat-frequency measurement facility, which permits two or three masers to be compared simultaneously. The masers' frequency synthesizers are offset from one another, and their receiver output signals are multiplied to 1.2 GHz and mixed in highly isolated double-balanced mixers. The periods of the resulting beat signals are measured by a three-channel, zero-deadtime counter and stored in a computer. Typically the frequency synthesizers are offset from one another by approximately 1.4 Hz at 1.42 GHz; after division to the 1.2 GHz comparison frequency, the beat frequency is approximately 1.18 Hz, corresponding to a beat period of approximately 0.84 s. When three masers are compared using

this system, one synthesizer is set approximately 1.4 Hz higher than the second, and the third approximately 1.4 Hz lower; thus the beat frequencies between the first and second masers and between the second and third masers are approximately 1.2 Hz, while the beat frequency between the first and third masers is approximately 2.4 Hz.

A second comparison system used at SAO is a time-difference measurement system[6] (TDMS). This system, which does not require synthesizer offsets, permits simultaneous phase comparisons of up to 24 clocks. For averaging times greater than roughly 10^4 s its measurement noise is below typical maser frequency instability, making it suitable for long-term comparisons.

In addition to comparisons by the TDMS, the relative phase of the Soviet masers was measured with the masers' one-pulse-per-second (1 pps) outputs. The time delay between the 1 pps signals was measured by a commercial time-interval counter and by a counter incorporated in Ch1-75.

The masers at SAO were compared with the external time scales by means of GPS common-view measurements. Throughout the observation period, Ch1-75's 5 MHz output provided the frequency reference for a GPS receiver located at SAO that was monitored via modem by NIST. These measurements related Ch1-75 to NIST's AT1 time scale; the measurements at SAO between Ch1-75 and the other masers at SAO then permitted comparison between the other masers and NIST(AT1).

NIST also carried out GPS common-view measurements with PTB and USNO (not indicated in Fig. 1). The USNO data linked the other clocks (at SAO, NIST, and PTB) to TAI and, by means of a TDMS at USNO, to the individual masers at USNO.

At the time the calculations reported here were made, TAI time was not available over the entire observation period; as a consequence we extrapolated TAI forward by means of hydrogen masers at USNO. To do this we characterized the masers at USNO in terms of their frequency drift and rate of change of drift relative to TAI over several months prior to modified Julian date (MJD) 48189, the last date for which TAI was available. The mathematical models used are given in Appendix A. The predicted times for the four most stable masers (N2, N4, P24, and P25) were then calculated forward to MJD 48215 using the models, and the average time was taken as representative of TAI for that period.

MEASUREMENT PROCEDURE

The Soviet masers were delivered to SAO on 24 September 1990. After they were installed in the Maser Laboratory's clock room and all of the masers had time to equilibrate, initial measurements were made from 28 September to 7 October to assess the masers and the measurement systems.

Formal measurements were carried out from 7 October to 28 November (MJD 48171 to 48223). Ch1-75's autotuning system, which is designed to improve its long-term frequency stability, was operated from 7 October to 16 November (MJD 48211). From 16 November to 28 November frequency comparisons were made with Ch1-75's autotuner off.

During the observation period the TDMS at SAO measured and recorded the phase of the masers at SAO at intervals of 500 s. The SAO beat comparison system measured the 0.84-s beat periods and calculated Allan deviations for averaging intervals of 0.84 s and longer; the beat period measurements were averaged in groups of 10 (84 s) and stored for later processing. The time interval between the Ch1-75 and Ch1-76 1-pps signals was recorded continuously on a chart recorder and measured digitally once per day. Both the TDMS and the beat system were interrupted occasionally for data backup and because of power-line spikes and software errors.

FREQUENCY VARIATION AS A FUNCTION OF TIME

The frequency behavior of clocks can be characterized by graphing pair-wise frequency differences as a function of time, and by plotting the Allan deviation, $\sigma_y(\tau)$, as a function of averaging interval τ. Figure 2 shows the time variation of Ch1-75's frequency against the primary frequency reference scales NIST(AT1), UTC(PTB), and TAI. The data are Kalman-smoothed estimates from GPS common-view measurements among the standards laboratories and SAO. Respective common-view measurement noises were 0.8 ns for TAI, 3 ns for UTC(PTB), and 2 ns for NIST(AT1). As discussed above, the TAI data were extrapolated forward by means of the masers at USNO. The general trends of Ch1-75 against the three time scales are consistent, indicating that the major frequency variations are due to Ch1-75 and that the scales are in good long-term agreement with one another.

NIST(AT1) was used as the independent standard frequency reference for estimating the frequency drifts of the masers at SAO. The frequency stability of NIST(AT1) is better than 10^{-14} for integration times of interest for this paper; its average frequency drift over the past few years with respect to either TAI or UTC(PTB) has been less than 1×10^{-16}/day. Annual variations of a few parts in 10^{14} have been observed between NIST(AT1) and UTC(PTB) or TAI. The source and cause of these variations have been studied but are not understood[7,8]. For the present work, the frequency drift of NIST(AT1) was estimated versus TAI and UTC(PTB) for the periods over which data were available and that best corresponded to our measurement period; these were MJD 48172 to 48215 for TAI (using the masers at USNO for extrapolation) and MJD 48172 to 48222 for UTC(PTB). Unfortunately, our measurements occur during what appears to be a period of steep annual frequency variation. The frequency drift of NIST(AT1) relative to TAI during the observation period was $+2.1\times10^{-16}$/day, and relative to UTC(PTB) was $+2.3\times10^{-16}$/day.

The frequencies of the masers at SAO against NIST(AT1) are shown in Fig. 3; their drift rates relative to NIST(AT1), calculated by means of linear regressions on the frequencies over the entire observation period, are given in Table 1. The Ch1-75–NIST(AT1) frequency difference was obtained from the GPS common-view measurements. The frequencies of P13 and P26 relative to NIST(AT1) were then calculated using the frequency differences between those masers and Ch1-75 measured by the SAO beat frequency measurement system; the values plotted represent one-hour averages observed once per day. Daily measurements of the Ch1-75–Ch1-76 time difference yielded the data for Ch1-76. The frequency excursions and subsequent recoveries seen in Fig. 3 for P13 and P26 at MJD 48201 were due to a two-hour power failure that affected those masers but not Ch1-75 or

Ch1-76. With the exception of the P13 and P26 excursions on MJD 48201, fluctuations that correlate among the data for Ch1-76, P26, and P13 are probably due to the GPS common-view time transfer or to NIST(AT1); such fluctuations, which appear across the data length, amount to roughly 1-2 ns per day, which is consistent with the level of previously observed common-view time transfer noise. The fluctuations are absent from the Ch1-75 graph because Ch1-75 was the clock controlling the GPS receiver, and its data were Kalman filtered with respect to NIST(AT1). The correlated fluctuations are difficult to identify in Ch1-76's frequency graph prior to MJD 48200, probably because they are obscured by Ch1-76's frequency variations.

Table 1
Drift rates of masers at SAO vs. NIST(AT1)

Maser	Frequency Drift (1×10^{-15}/day)
Ch1-75	–8.6
Ch1-76	–3.1
P13	+0.7
P26	+9.6

The frequency of Ch1-75 versus P26 is shown in Fig. 4. A frequency offset of roughly 1×10^{-11} has been removed for convenience in plotting. The two spikes at MJD 48215 and MJD 48221, which correspond to phase jumps of about 0.5 ns, were apparently caused by the time-difference measurement system; they did not appear in data from the beat-frequency system. Ch1-75's autotuner, which operated until 16 October (MJD 48211), clearly adds short- and intermediate-term frequency instability. Within the confidence of estimate of the data of Figs. 2–4, Ch1-75's drift seems unaffected by the operation of its autotuner. The two-month test is probably too short to establish with confidence the autotuner's long-term effect on Ch1-75's frequency.

FREQUENCY STABILITY

Short-term frequency stability measurements of the active masers at SAO, as expressed by the Allan deviation $\sigma_y(\tau)$, were obtained from the beat-frequency measurements system and are shown in Fig. 5. The measure used in Fig. 5 is the reduced Allan deviation, $\tilde{\sigma}_y(\tau) \equiv \sigma_y(\tau)/\sqrt{2}$, for the frequency pair. If two oscillators contribute equal amounts of noise, then $\tilde{\sigma}_y(\tau)$ represents the frequency variability of the individual oscillators; if, however, one oscillator contributes considerably more noise than the other, as in the case of Ch1-75 with autotuner on, then $\sigma_y(\tau)$, rather than $\tilde{\sigma}_y(\tau)$, represents the variability of the noisier oscillator. Figure 5 gives $\tilde{\sigma}_y(\tau)$ for the frequency differences P26–Ch1-75 and P26–P13 over two nine-day intervals. During interval A, 11 October – 20 October (MJD 48175 – 48184), Ch1-75's autotuner was operating; during interval B, 16 October – 25 October (MJD 48211 – 48220), the autotuner was turned off. By the beginning of interval B, P13 and P26 had restabilized following the power interruption on 6 November. Curves *a* and *b* in Fig. 5 show the stability of P26 vs Ch1-75 with the autotuner on and off (during intervals A and B), respectively. A relative drift of 1.68×10^{-14}/day has been removed from curve *a*, and a drift of 1.24×10^{-14}/day from curve *b*. The peak in curve *a* at approximately τ=100 s probably results from

modulation of Ch1-75's internal magnetic field at a period of 100 s for the autotuner. Curve *c* is the reduced Allan deviation for P26–P13 during interval B; a relative drift of 6.45×10^{-15}/day has been removed. The drift-removed stability of P26–P13 during interval A was not significantly different from curve *c*. The effect of removing frequency drift is seen by comparison with curve *d*, which gives the reduced Allan deviation for P26–P13 without drift removal. Curves *b* and *c* show that the drift-removed stability levels of the Soviet (autotuner–off) and SAO masers are comparable for averaging times between a second and a day.

Comparison of $\tilde{\sigma}_y(\tau)$ with the line segments included in Fig. 5 shows that $\tilde{\sigma}_y(\tau)$ [and thus $\sigma_y(\tau)$] is proportional to τ^{-1} for $\tau<100$ s and to $\tau^{-1/2}$ for $100<\tau<7\times10^3$ s; as predicted theoretically[9], this behavior is due to additive noise in the maser receivers and noise within the atomic linewidth, respectively. For $\tau>10^4$ s, $\tilde{\sigma}_y(\tau)$ is proportional to τ^1 for P26–P13 with drift not removed; this form of $\tilde{\sigma}_y(\tau)$ is characteristic of linear frequency drift. In the case of the drift-removed data, portions of the graphs are approximately proportional to $\tau^{1/2}$, which is identified with random walk of frequency; this behavior may result from the simultaneous action of several quasi-independent frequency-determining mechanisms in the masers.

The long-term frequency stability of Ch1-75 against the three time scales, with drift removed, is shown in Fig. 6. (In Figs. 6–11 the Allan deviation $\sigma_y(\tau)$ is used, rather than the reduced deviation $\tilde{\sigma}_y(\tau)$.) The data for AT1 and PTB cover the entire observation period, MJD 48171 to 48223, while the TAI values cover MJD 48171 to 48215. Due to the Kalman filtering, the values for 1- and 2-day averaging intervals are artificially low, by perhaps a factor of 2; however, the data for $\tau\geq4$ days are representative of the performance of the clocks. That the drift rate for Ch1-75 against TAI is greater than the rates against AT1 and PTB may be due to the fact that the shorter time span over which the TAI data were available corresponded to an interval during which Ch1-75's drift was greater than its average value for the entire observation period. The Allan deviation of the three scales relative to one another is shown in Fig. 7. The stability of AT1 versus TAI, in particular, is considerably lower than the values in Fig. 6, indicating that the latter values represent the stability of Ch1-75.

The long-term stabilities of the clocks at SAO are shown in Fig. 8. The data were obtained from the TDMS at SAO, with interruptions spanned by linear interpolation. The calculations for Ch1-75–P13 and for P26–P13 are based on frequency data obtained from MJD 215.8 to 221.7; those for Ch1-75–P26, on data taken from MJD 211.5 to 223.7; and those for Ch1-75–Ch1-76, on data taken from MJD 204.9 to 223.8. Thus the plots not involving Ch1-76 represent data taken with Ch1-75's autotuner not operating, while the Ch1-75–Ch1-76 plot includes data with Ch1-75's autotuner both on and off; however, because Ch1-76's stability is considerably less than that of Ch1-75, $\sigma_y(\tau)$ for the Ch1-76–Ch1-75 frequency difference is not significantly affected by the operation of Ch1-75's autotuner.

Figures 9 and 10 show the stabilities of the individual masers at USNO in the ensemble used to extrapolate TAI. $\sigma_y(\tau)$ was obtained for each clock from an N-cornered hat calculation from the Allan variance of the frequency differences with frequency drift and rate-of-change of drift removed. The stability of a cesium clock with little frequency drift is included for comparison. Although the N-cornered hat procedure is theoretically exact for population variances, in practice it yields differences

between pairs of sample variances observed over finite times; consequently, the calculated variances σ_y^2 for the best clocks of the group can (randomly) be negative numbers, which are omitted in Figs. 9 and 10. The least stable clocks of the group are well characterized, while for the most stable clocks, N2, N4, N5, P24, and P25, one can say only that their stabilities are below 1×10^{-15} for intervals from 10^5 s to 3×10^6 s.

DISCUSSION

From the observations presented here, it is apparent that maser frequency stabilities of a few parts in 10^{15} and below are achieved for averaging intervals from one day to about two weeks, levels that are an order of magnitude lower than those attained perhaps ten years ago. These stabilities require removal of frequency drift and, in some cases, rate of change of drift.

The frequency prediction capability of hydrogen masers seems to be somewhat better than 10^{-14} for extrapolation over a few weeks. In our case, the forward prediction from MJD 48189 to 48218 showed modelling errors of less than 1×10^{-14}, and for some masers a few parts in 10^{15}. The prediction errors were calculated by subtracting the frequency residuals between different pairs of USNO masers after removing their respective parameterized models. Figure 11 shows the residual errors between four pairs of masers, expressed in terms of $\sigma_y(\tau)$ calculated from MJD 48172 to 48218; these results demonstrate unprecedented oscillator predictability.

The time scale instabilities evident in Fig. 7, of about 10^{-14} at one day intervals, are due principally to the cesium standards involved. Our drift-removed data show about an order-of-magnitude advantage of hydrogen masers over cesium devices at integration times of one day.

ACKNOWLEDGEMENTS

We thank the Frequency and Timing Engineering group of the NASA Jet Propulsion Laboratory for enabling us to include maser P26 in this comparison; Mr. Lee Erb for the loan of measurement equipment; Dr. Marc Weiss, Mr. Tom Weissert, and Ms. Trudi Peppler (NIST) and Dr. Lee Breakiron (USNO) for assistance with data analysis; and Mr. Richard Nicoll and Mr. Donald Graveline (SAO) and Mr. Sergei Kozlov and Mr. Gherman Chernov ("Quartz" Research) for assistance with maser setup and operation. We are grateful to the Smithsonian Institution for its support of the activity at SAO.

APPENDIX A -- EXTRAPOLATION OF TAI TIME SCALE

At the time this analyis was done, the time differences between UTC(USNO) and TAI were available only through MJD 48189. The TAI time scale was represented over the entire observation period (MJD 48172 to 48215) by modelling hydrogen masers at USNO over periods prior to MJD 48189 during which they were well characterized against the known values of TAI, and extending the models to MJD 48215. Since each of the masers is measured against UTC(USNO), they can be related to TAI through the TAI–UTC(USNO) time difference data. Each maser was modelled by a three-parameter expression,

$$y(n) = [C_0 + C_1 n + C_2 n^2] \times 10^{-15} \quad (1)$$

Here $y(n) = y_{maser} - y_{TAI}$ is the normalized frequency offset of the maser from TAI at day n, where n is the day count relative to the reference date given in Table 2. C1 is the maser's frequency drift rate, and C2 its rate of change of frequency drift, relative to TAI. N in Table 2 is the number of frequency measurements, each representing a 10-day average, used to establish the coefficients from BIPM circular-T 10-day data. Masers N2–N5 use cavity autotuning systems that employ modulation of the cavity resonance frequency[5]; masers P18–P25 do not use cavity autotuning.

Table 2
Parameters of model for USNO masers vs. TAI

Clock	Reference Date	C_0	C_1	C_2	N	Rms of residuals (10^{-15})
N2	48024	–1199.1	1.21	–0.003	34	15.5
N3	48159	–1190.1	0.01	----	6	3.0
N4	48174	550.5	–0.20	----	4	2.9
N5	48164	212.7	0.16	----	6	11.0
P18	48039	–82.2	0.62	----	31	12.3
P19	48099	–9.8	2.15	–0.004	19	8.8
P23	48129	–125.3	1.62	–0.008	13	11.1
P24	48029	7684.0	3.20	–0.006	33	15.1
P25	48129	784.4	5.12	–0.012	13	9.6
Cs2485	48074	922.2	0.057	----	24	18.1

REFERENCES

1 B.A. Gaygerov, L.P. Yelkina and S.B. Pushkin, "Metrological characteristics of a group of hydrogen clocks." *Measurment Technology* **25**, 23 (1982).

2 N.A. Demidov and A.A. Uljanov, "Design and industrial production of frequency standards in the USSR." *Proc. 22nd Precise Time and Time Interval (PTTI) Applications and Planning Meeting* (this issue) (1990).

3 A.A. Belyaev, N.A. Demidov, B.A. Sakharov, V.Yu. Maksimov, M. Yu. Fedotov, and A.E. Yampol'skii, "Ch1-76 small-size passive hydrogen frequency and time." *Measurement Techniques* **30**, 767 (1987).

4 E. M. Mattison and R. F. C. Vessot, "Performance of model VLG-12 advanced hydrogen masers." *Proc. 44th Annual Freq. Control Symposium*, p. 66 (1990)

[5] H.E. Peters, H.B. Owings, and P.A. Koppang, "Atomic hydrogen masers with self auto-tune system and magnetic field cancellation servo." *Proc. 20th Annual Precise Time and Time Interval (PTTI) Applications and Planning Meeting*, p. 337 (1988)

[6] Erbtec Corporation, Boulder, Colorado.

[7] D.W. Allan, "A study of long-term stability of atomic clocks." *Proc. 19th Annual Precise Time and Time Interval (PTTI) Applications and Planning Meeting*, p. 375 (1987).

[8] D.W. Allan, M.A. Weiss, and T.K. Peppler, "In search of the best clock." *IEEE Trans. Inst. and Meas.* 38, 624 (1989).

[9] R.F.C. Vessot, M.W. Levine, and E.M. Mattison, "Comparison of theoretical and observed hydrogen maser stability limitation due to thermal noise and the prospect for improvement by low-temperature operation." *Proc. 9th Annual Precise Time and Time Interval (PTTI) Applications and Planning Meeting*, p. 549 (1977).

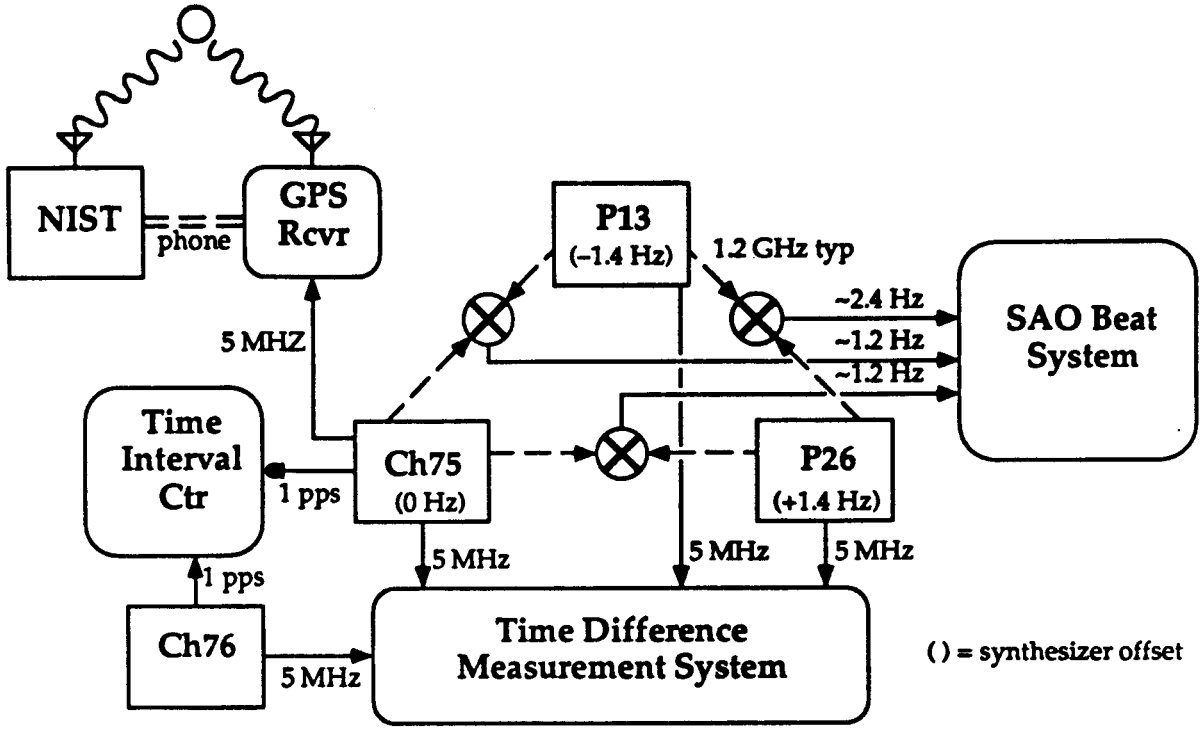

Fig. 1a. Comparison systems at SAO with Ch1-75 autotuner off

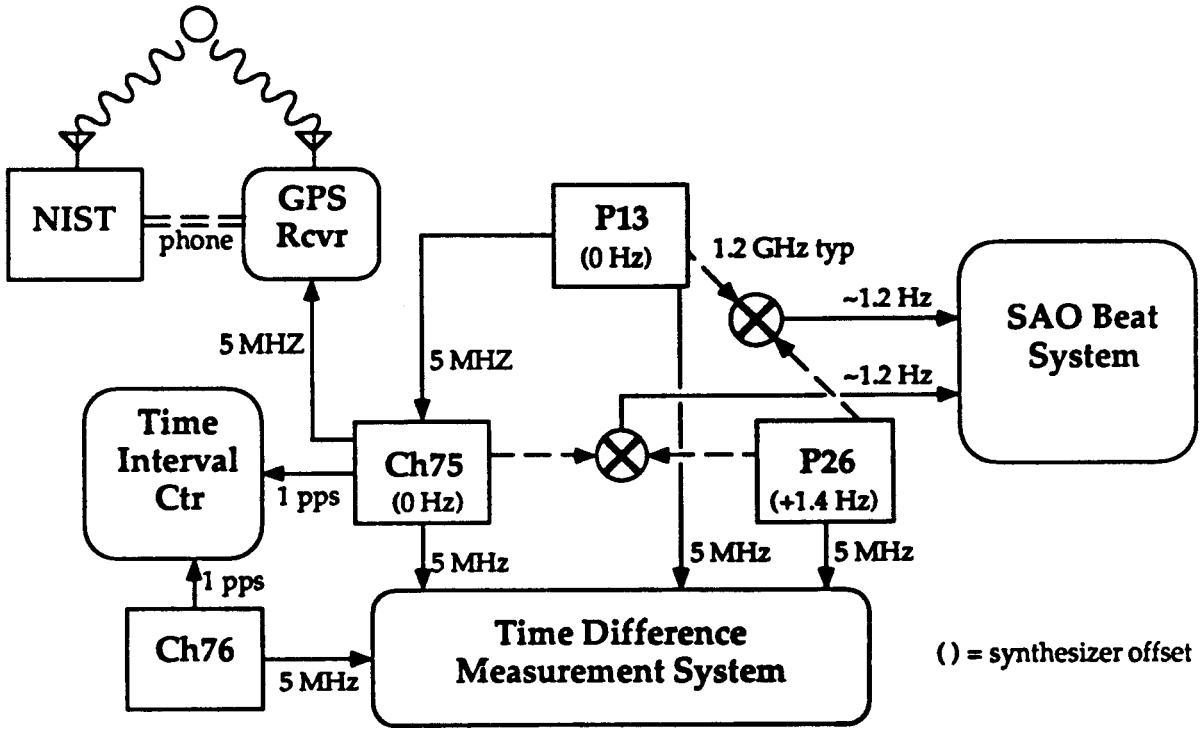

Fig. 1b. Comparison systems at SAO with Ch1-75 autotuner on

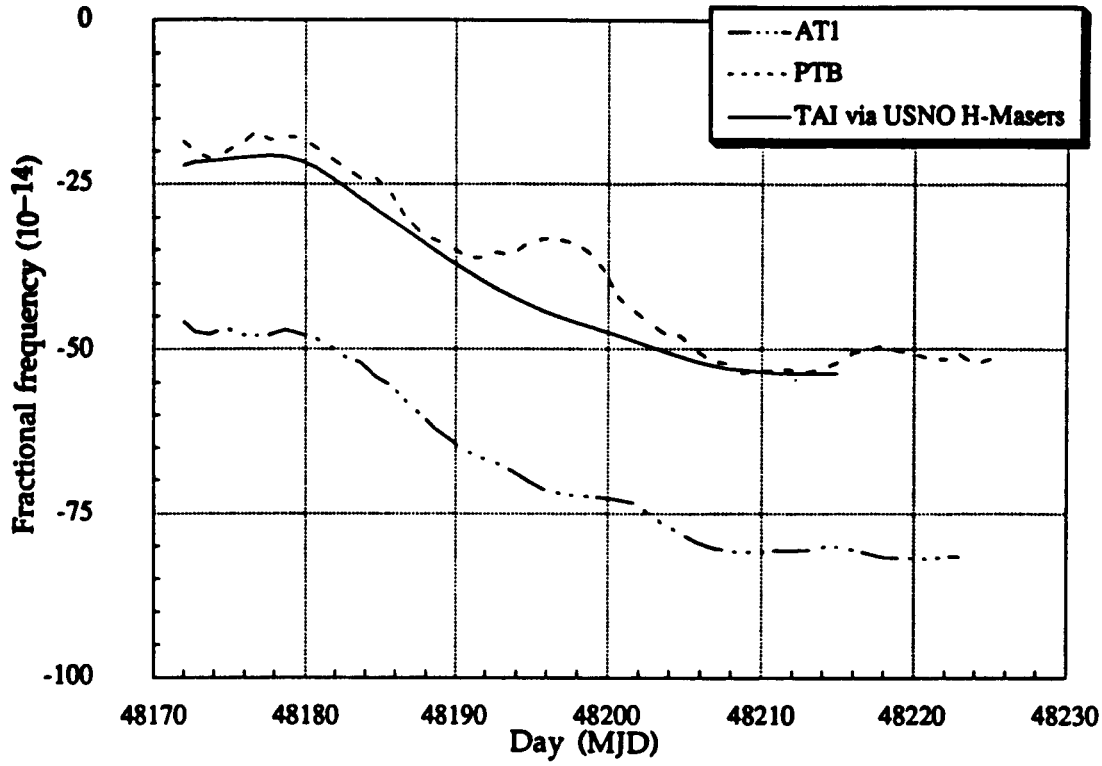

Fig. 2. Frequency of Ch1-75 relative to principal frequency standards (Kalman smoothed)

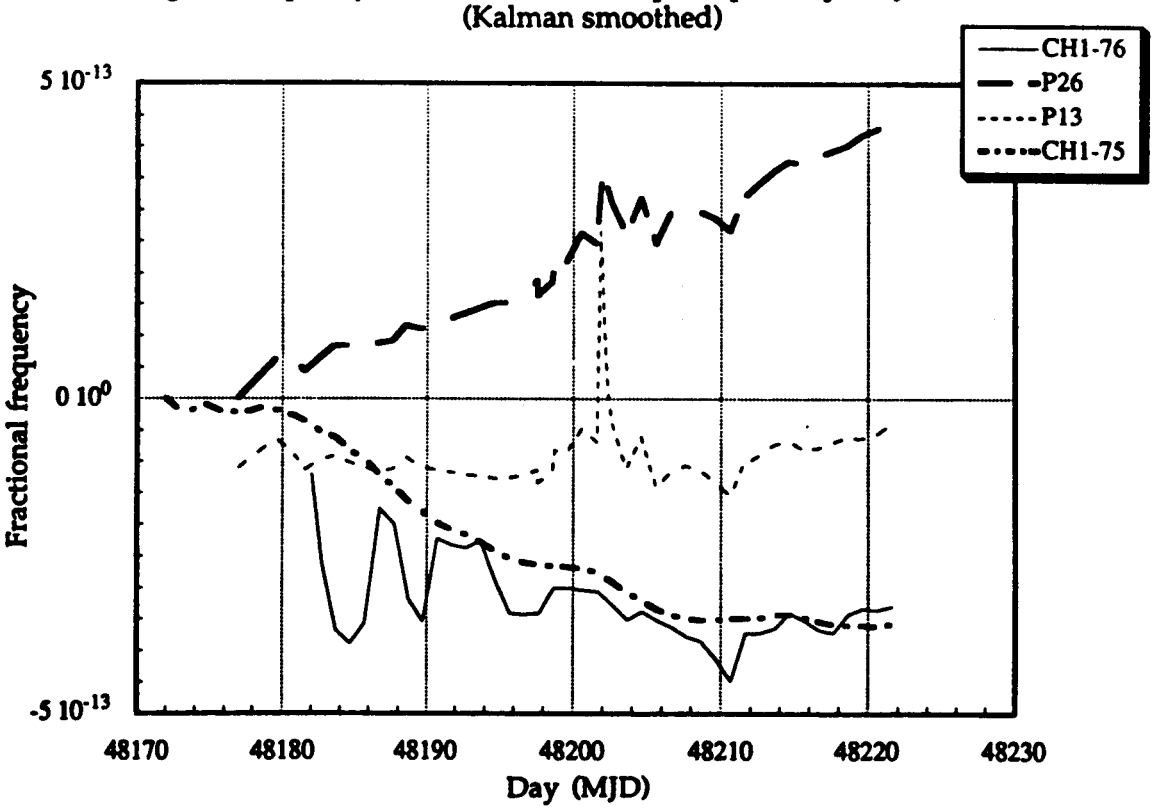

Fig. 3. Frequencies of masers at SAO vs. NIST(AT1)

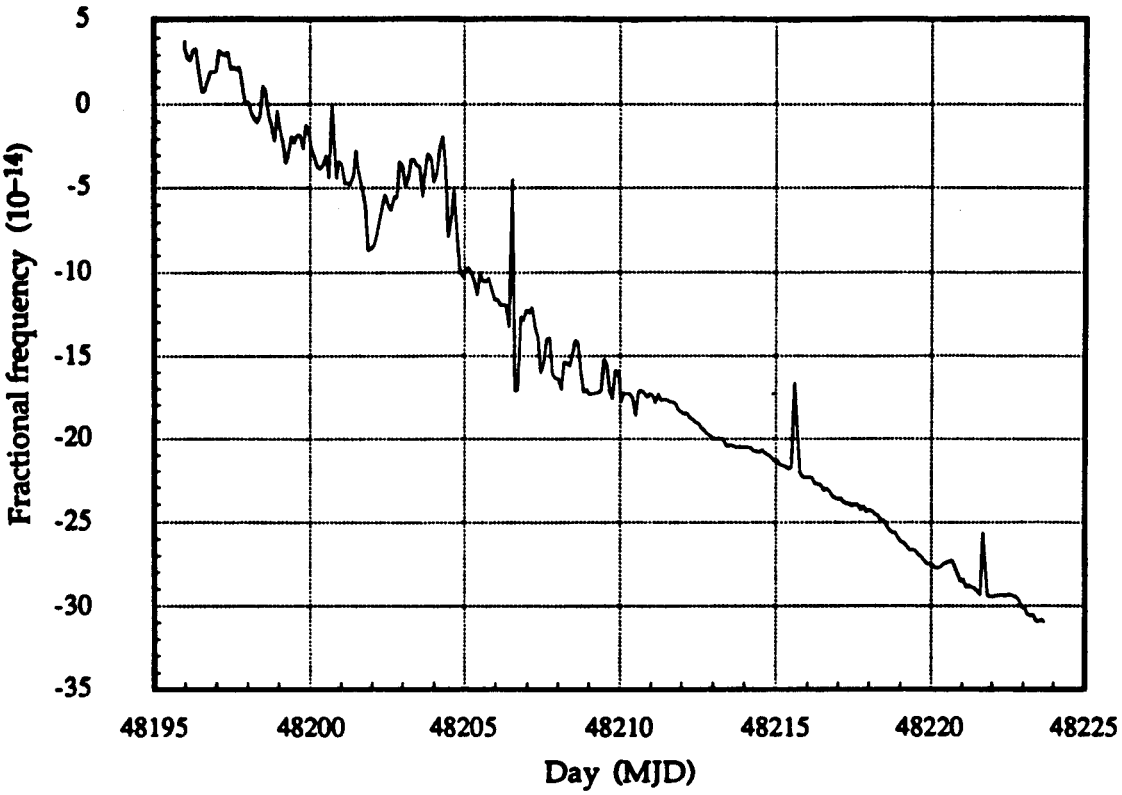

Fig. 4. Frequency difference of Ch1-75 vs. P26

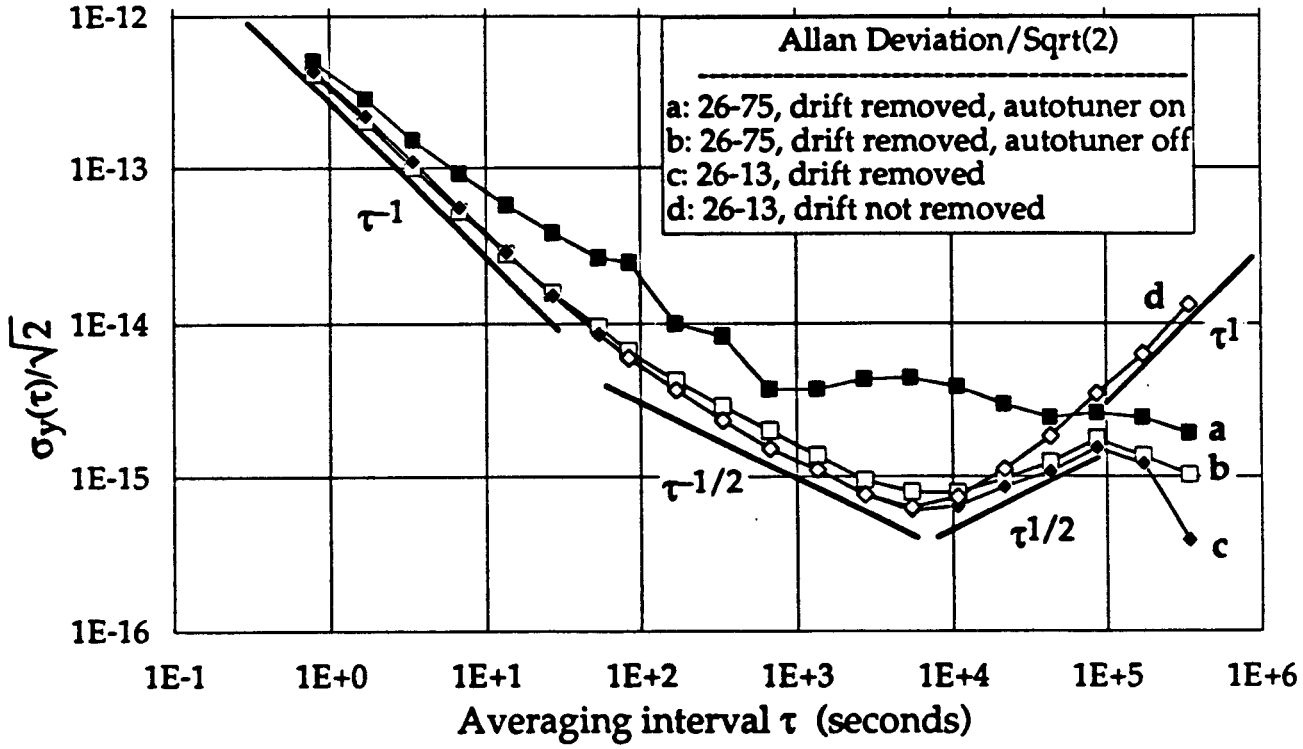

Fig. 5. Frequency stabilities of masers at SAO

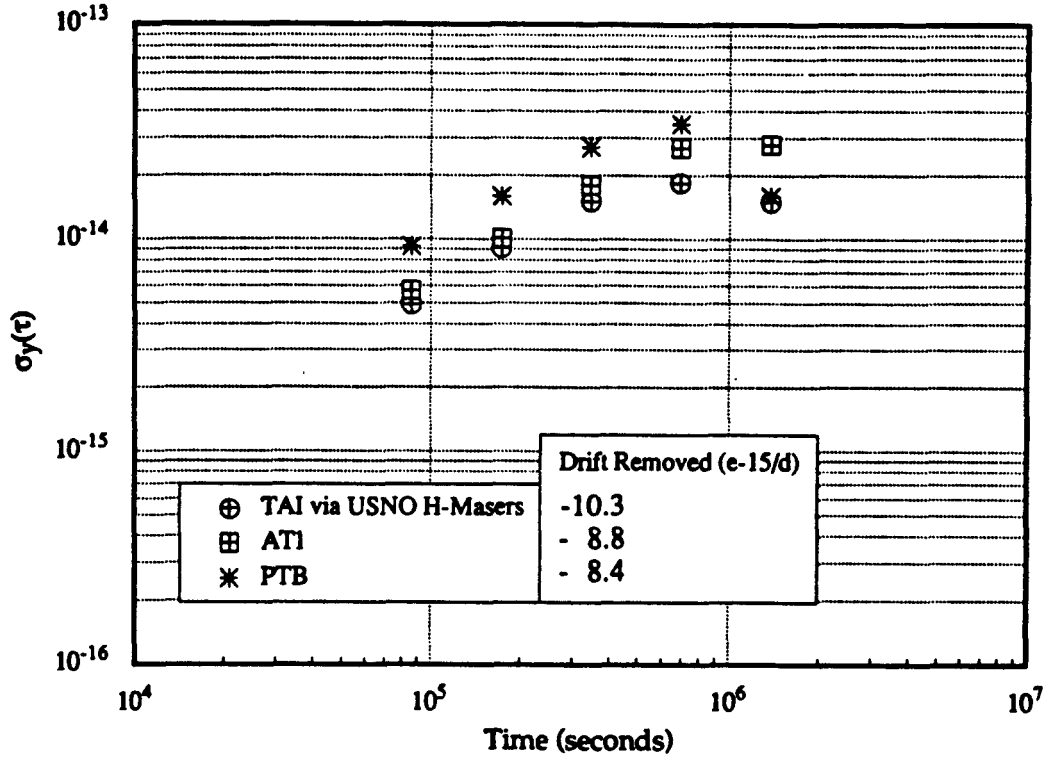

Fig. 6. Frequency stabilities of Ch1-75 vs. frequency standards (Kalman smoothed)

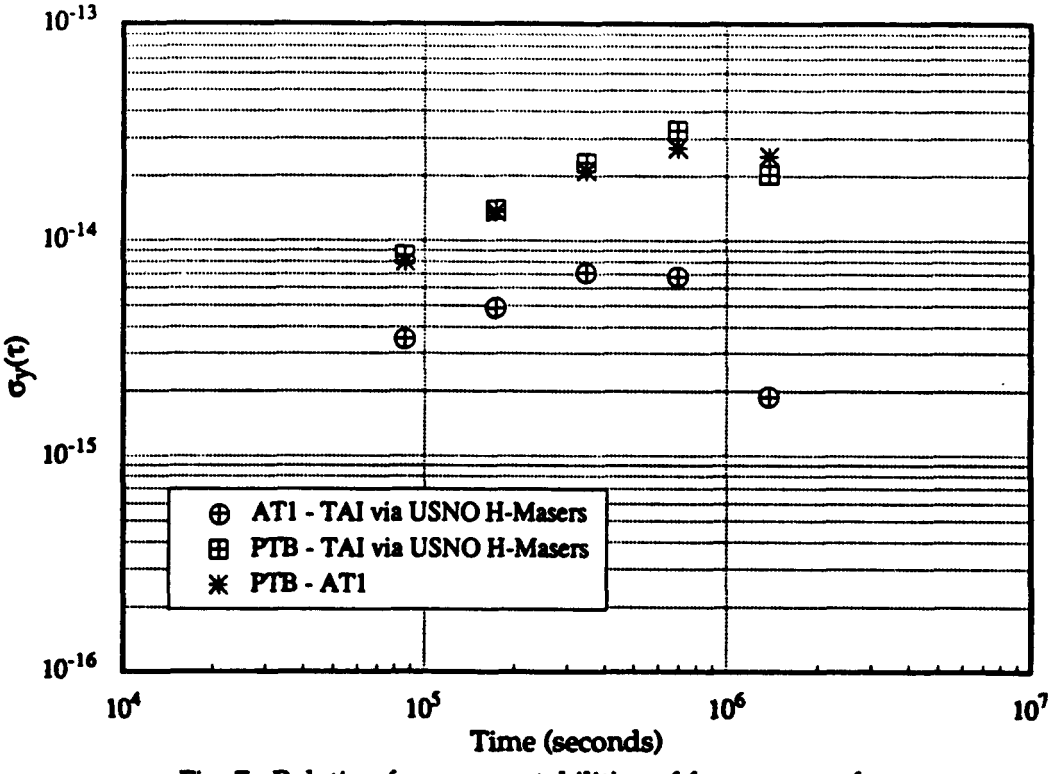

Fig. 7. Relative frequency stabilities of frequency references (Kalman smoothed)

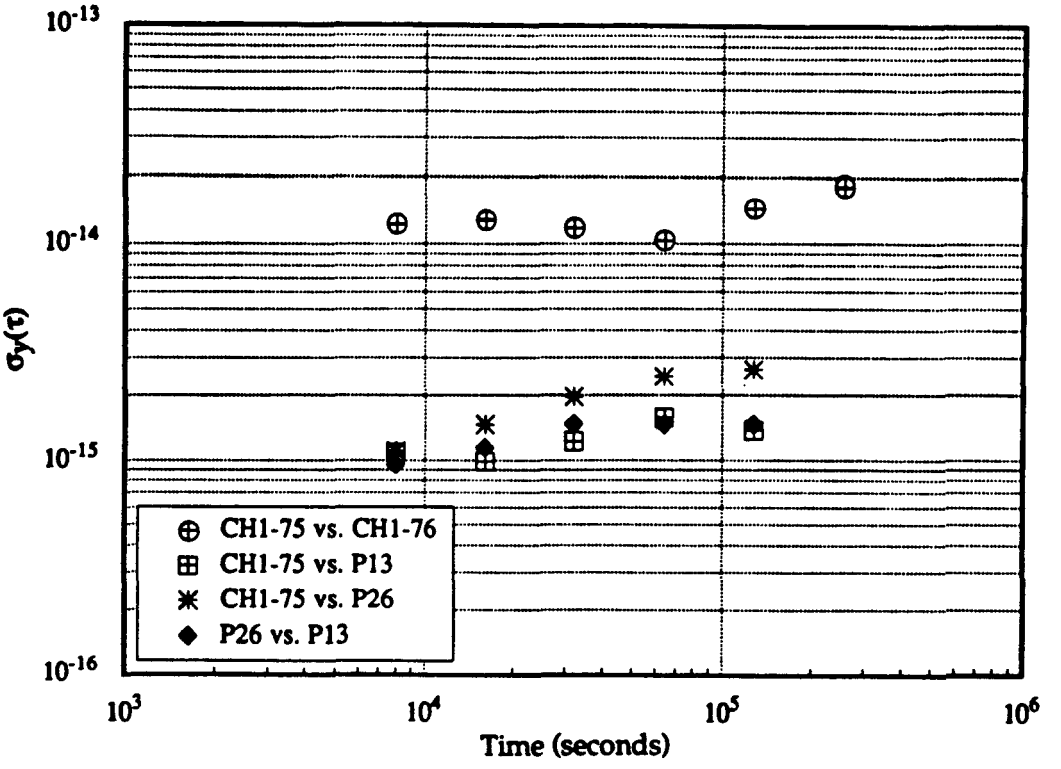

Fig. 8. Relative frequency stabilities of masers at SAO (drift removed)

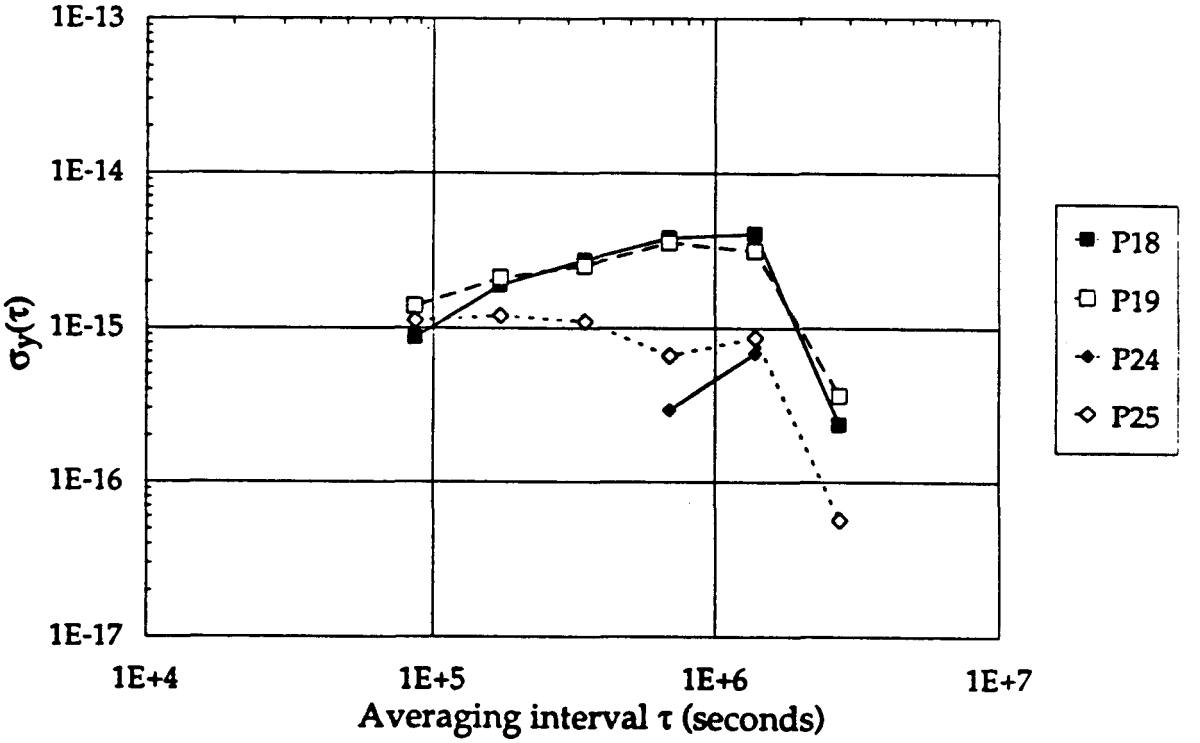

Fig. 9. Frequency stabilities of masers at USNO, from N-corner hat calculation

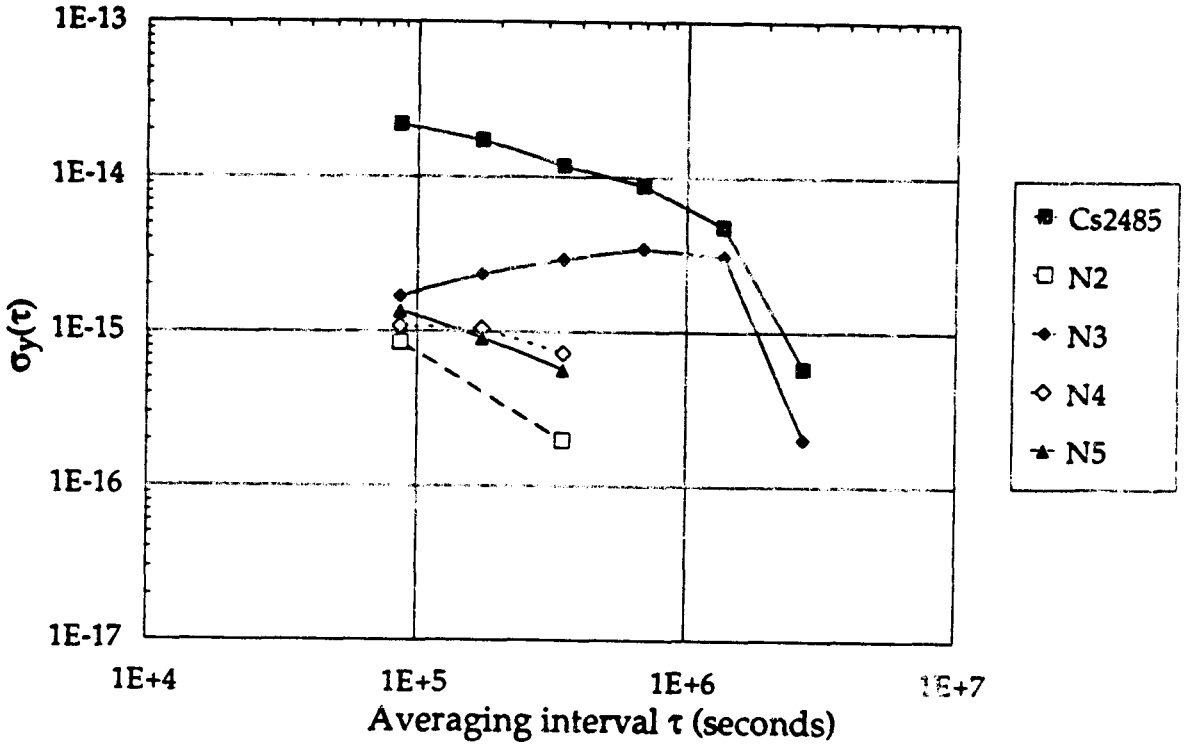

Fig.10. Frequency stabilities of masers and cesium clock at USNO, from N-corner hat calculation

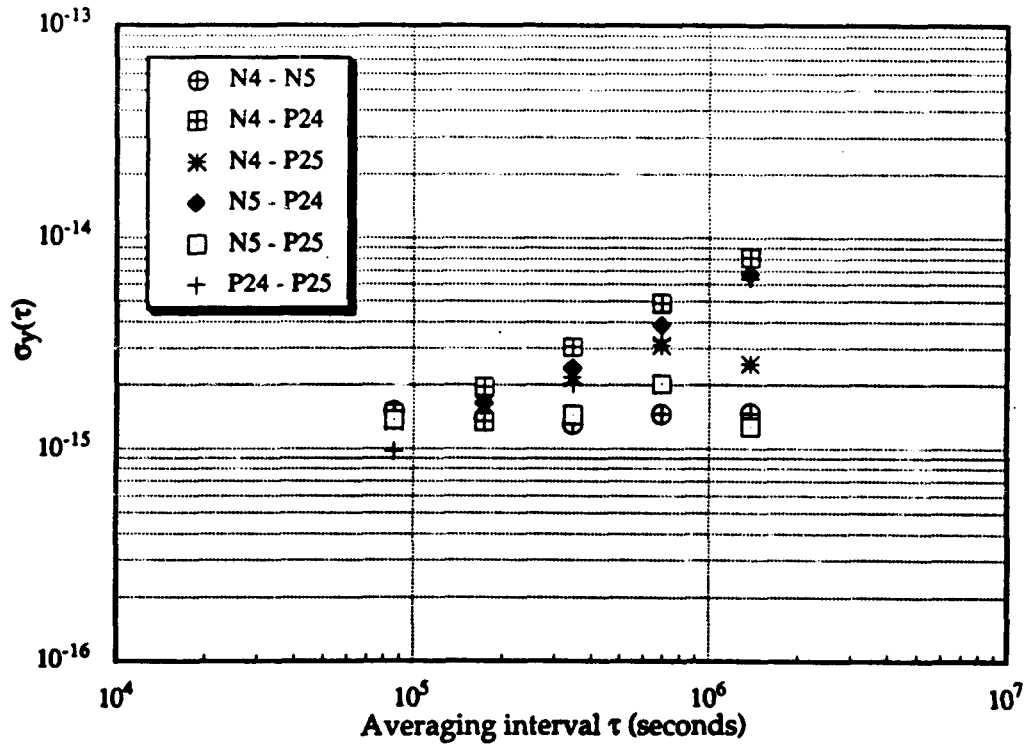

Fig. 11. Pair-wise stabilities of frequency residuals of 4 masers at USNO, with clock models removed